



Published in final edited form as:

JACC Adv. 2024 January ; 3(1): . doi:10.1016/j.jacadv.2023.100740.

Cardiac Radiomics Are Associated With Dyspnea

Saurabh Kumar, PhD^{a,b}, Sadeer Al-Kindi, MD^c, Mohamed H.E. Makhoul, MD^c, Shruti Sivakumar, PhD^a, Abhishek Midya, PhD^{a,b}, Gourav Modanwal, PhD^{a,b}, Varun Rajagopalan, MD^d, Animesh Tandon, MD, MS^e, Sanjay Rajagopalan, MD^{c,‡,†}, Anant Madabhushi, PhD^{a,b,‡,*}

^aCase Western Reserve University, Cleveland, Ohio, USA;

^bSchool of Medicine, Emory University, Atlanta, Georgia, USA;

^cSchool of Medicine, Case Western Reserve University, Cleveland, Ohio, USA;

^dUniversity Hospitals, Cleveland, Ohio, USA;

^eCleveland Clinic, Cleveland, Ohio, USA.

Unexplained dyspnea is common in patients with chronic human immunodeficiency virus (HIV) infection and may represent a consequence of chronic subclinical cardiac abnormalities especially heart failure with preserved ejection fraction. Cardiac magnetic resonance (CMR) imaging offers a unique opportunity to investigate myocardial structure, function and mechanics, which may be implicated in the development of heart failure. Recently, machine learning techniques have allowed more complex analysis of spatial and temporal information contained in CMR data that could help facilitate prediction of adverse cardiovascular outcomes. Accordingly, to understand the role of subclinical myocardial abnormalities in development of exercise intolerance, we sought to investigate the contribution of computationally-derived CMR-based cardiac structure and mechanics to objective measures of exercise intolerance in patients with HIV.

We performed an analysis of patients from a prospective cohort of 51 people living with HIV (age 50.4 ± 1.7 years, body mass index 30.5 ± 1.0 kg/m², years of HIV exposure 19.7 ± 1.7 years, and absolute CD4 count 791 ± 69 cells/ μ L) without overt hypertension or prior cardiovascular disease with dyspnea (defined as grade 2 or 3 on the modified Medical Research Council scale [33040733]).¹ All subjects were without evidence of gross cardiac or pulmonary abnormalities by resting echocardiography, chest x-ray, or chest CT scanning. Short-axis cine resting CMR scans were obtained on a 1.5-T MRI (Siemens, Espree) covering both ventricles from base to apex (slice thickness of 10 mm and interslice gap of 2 mm). During maximal cardiopulmonary exercise testing, the patients were encouraged to exercise to exhaustion, defined by a respiratory exchange ratio >1.0 . Metabolic gas exchange

THIS IS AN OPEN ACCESS ARTICLE UNDER THE CC BY-NC-ND LICENSE (<http://creativecommons.org/licenses/by-nc-nd/4.0/>).

^{*}Emory University School of Medicine, 100 Woodruff Circle, Atlanta, Georgia 30322, USA. anantm@emory.edu. [†]Division of Cardiovascular Medicine University Hospitals, 11100 Euclid Avenue, Suite 1800 Cleveland Ohio 44106, USA, sanjay.rajagopalan@uhhospitals.org.

[‡]Drs Rajagopalan and Madabhushi are co-senior authors.

measures including peak oxygen consumption (PkVO₂) were measured both during rest and stress. This study was approved by University Hospitals Institutional Review Board, and all participants provided informed consent prior to enrollment.

The left ventricle (LV) and LV myocardium (LVMC) were segmented using a pretrained UNet model² followed by manual fine-tuning by an expert cardiologist (Figure 1A). This was followed by extraction of 2D and 3D shape and texture features during a cardiac cycle including the end-systole and end-diastole. We extracted a total of 162 2D and 3D shape and morphology features and 824 3D-texture features (Figure 1B) such as raw intensities, Gray, Gabor, Laws energy, gradient, and entropy-based features (median, variance, kurtosis, and skewness of 103 features for both LV and LVMC at end-diastole and end-systole phases). The expression values of the features show significant between-patient variance (Figure 1C). A clustered heatmap (Figure 1D) illustrates the correlation between features that had the highest linear correlation with percent predicted PeakVO₂ (pp-PkVO₂). To avoid overfitting, we selected only 6 features and ensured that there was no multicollinearity between them (VIF <5). A multivariate linear regression model, which utilized 6 features including age, LV shape, and LVMC texture features (Figure 1E), demonstrated a moderate ability to predict pp-PkVO₂ with an R^2 value of 0.37 ± 0.03 in 100 bootstrapped validation sets. By averaging the coefficients from these 100 iterations, we achieved an improved prediction of pp-PkVO₂ with an R^2 value of 0.61 (Figure 1F). The entire analysis was conducted using Python 3.8.

In this proof-of-concept analysis, we show that a combination of CMR shape and texture radiomics can explain 61% of variation in pp-PkVO₂ in patients with HIV and unexplained dyspnea with otherwise no overt cardiopulmonary abnormalities. Shape features such as median LV sphericity and standard deviation of LV aspect ratio capture the dynamic behavior of the LV and provide insights into its pumping function during the cardiac cycle. Texture features such as skewness and kurtosis derived from Gabor, Laws, and gradient transformations reflect the spatial variations and intensity patterns within the myocardium, shedding light on underlying microstructural changes related to tissue composition. Prior studies have suggested that people living with HIV have higher rates of fatigue and exercise intolerance compared with uninfected controls. In the general population, exercise tolerance³ and peak oxygen consumption are strongly associated with heart failure and heart failure-related long-term mortality.⁴ Our study suggests that novel radiomic markers of myocardial kinetics noted on resting CMR may be associated with exercise intolerance and may be helpful to predict adverse cardiac outcomes such as heart failure. Our approach could reduce the need for peak exercise and cardiopulmonary exercise testing, thereby reducing patient discomfort and examination costs. Prior studies have investigated the role of CMR-derived radiomics to predict cardiovascular outcomes. Pujadas et al. recently showed that a combination of clinical risk factors, CMR-derived radiomics can predict incident heart failure in the UK biobank (accuracy 0.77, area under curve 0.83).⁵ Collectively, the data suggests that CMR-derived radiomics may provide additional information not available in routinely collected clinical or CMR-derived data. Given the limitations of the study including lack of external validation, additional validation in a larger external cohort and association with long-term outcomes is warranted.

Acknowledgments

Dr Madabhushi is an equity holder in Picture Health, Elucid Bioimaging, and Inspirata Inc; serves on the advisory board of Picture Health, Aiforia Inc, and SimBioSys; currently consults for SimBioSys; has sponsored research agreements with AstraZeneca, Boehringer-Ingelheim, Eli-Lilly, and Bristol Myers-Squibb; his technology has been licensed to Picture Health and Elucid Bioimaging; and is involved in 3 different R01 grants with Inspirata Inc. All other authors have reported that they have no relationships relevant to the contents of this paper to disclose. The authors attest they are in compliance with human studies committees and animal welfare regulations of the authors' institutions and Food and Drug Administration guidelines, including patient consent where appropriate. For more information, visit the [Author Center](#).

REFERENCES

1. Mahler DA, Wells CK. Evaluation of clinical methods for rating dyspnea. *Chest*. 1988;93:580–586. [PubMed: 3342669]
2. Isensee F, Jaeger PF, Kohl SAA, et al. nnU-Net: a self-configuring method for deep learning-based biomedical image segmentation. *Nat Methods*. 2021;18:203–211. [PubMed: 33288961]
3. Weibel AR, Jenkins T, Longenecker C, et al. Relationship of HIV Status and fatigue, cardiorespiratory fitness, myokines, and physical activity. *J Assoc Nurses AIDS Care*. 2019;30(4):392–404. [PubMed: 31241504]
4. Setor KK, Sudhir K, Hassan K, et al. Associations of cardiovascular and all-cause mortality events with oxygen uptake at ventilatory threshold. *Int J Cardiol*. 2017;236:444–450. [PubMed: 28209387]
5. Pujadas ER, Raisi-Estabragh Z, Szabo L, et al. Prediction of incident cardiovascular events using machine learning and CMR radiomics. *Eur Radiol*. 2022;33(5):3488–3500. [PubMed: 36512045]

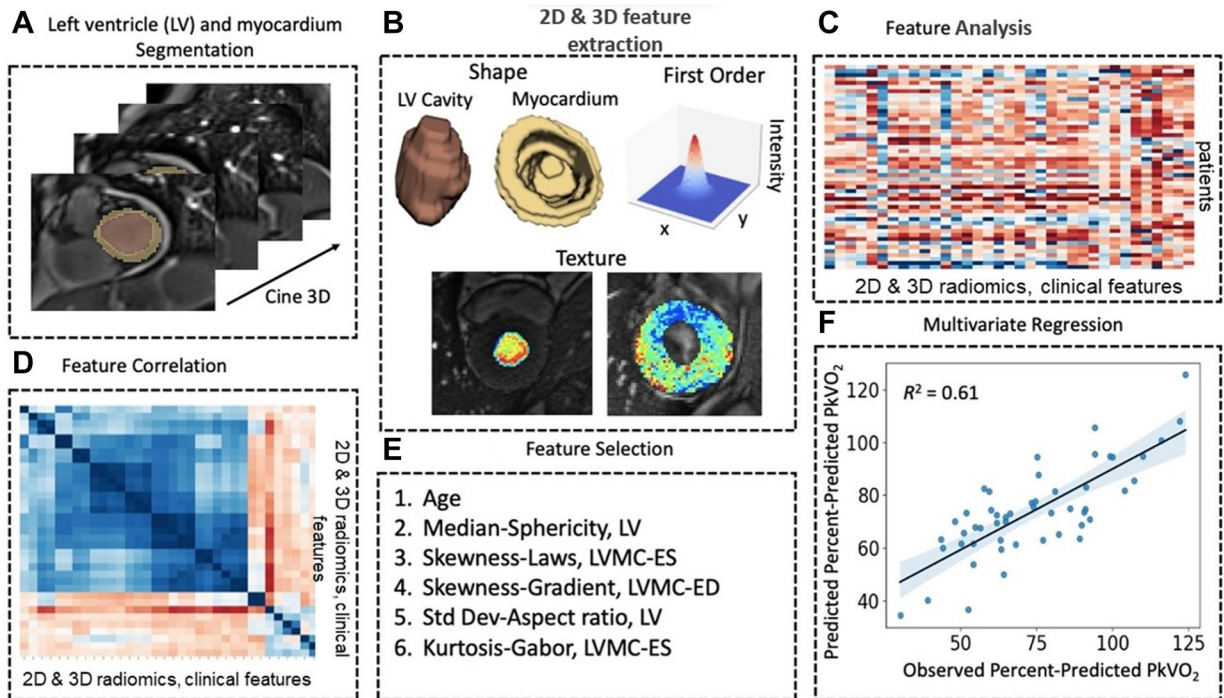


FIGURE 1. Computational Pipeline to Derive a CMR-Derived Risk Score to Predict Pp-Peak VO_2

(A) Stack of real-time cine images in the short-axis plane with slice thickness of 10 mm covering both ventricles from base to apex. Segmentations of LV and myocardium were obtained by a pretrained deep learning network, which were further improved upon manually. (B) Illustration of 3D shapes of the LV cavity and the myocardium, first-order features, and texture features. (C) Heatmap showing expression values of the 162 shape and 824 texture features extracted for each of the 51 patients with notable between-patient variance. (D) Clustered heatmap showing correlation between the 104 features that had the highest linear correlation with Pp-Pk VO_2 . (E) The final set of minimally correlated features (variance inflation factor <5) that were used to predict Pp-Pk VO_2 . (F) Scatter plot with 95% confidence interval between the observed and predicted Pp-Pk VO_2 values. The model used was the average of 100 models trained on 80% of the entire dataset drawn randomly with replacement. CMR = cardiac magnetic resonance; LV = left ventricle.